Spectral and temporal modifications of a weak resonant ultrashort pulse propagating in a two-level system driven by a strong nonresonant field

J. C. Delagnes, F. A. Hashmi, and M. A. Bouchene
Laboratoire de Collisions Agrégats Réactivité, C.N.R.S. UMR 5589, IRSAMC, Université Paul Sabatier, 118 Route de Narbonne, 31062 Toulouse Cedex 4, France

(Received 7 February 2006; published 30 November 2006)

An ultrashort strong nonresonant pulse induces transient phenomena in an optically thick medium consisting of an ensemble of nondegenerate two-level atoms (nonadiabatic transitions, transient light-shifts,...). A weak resonant pulse propagates in the system and we study theoretically and numerically the temporal and spectral modifications that are induced. Moreover, we show that the atomic media, modified by a strong pulse can act as a "pulse-shaper" device that can modify, in a controlled way, the shape of the weak pulse. It maps out the transient light shift induced by the strong pulse and reduces efficiently the long time dispersion tail of the weak pulse. We study and discuss the physical phenomena that allow such shaping effects and the necessary conditions to satisfy in order to observe them.

DOI: 10.1103/PhysRevA.74.053822 PACS number(s): 42.65.Re, 42.50.Gy, 42.50.Hz, 42.50.Md

I. INTRODUCTION

A lot of theoretical and experimental work on the dynamics of a two-level system driven by a strong field has been accumulated. A whole range of new phenomena has been predicted and later experimentally verified. Rabi oscillations [1], adiabatic following [2], and Mollow triplet of fluorescence [3] are some to name in the case when a strong field interacts with a two-level system. In the case of nonresonant ultrashort pulses, phenomena like nonadiabatic transitions and transient light shifts play a crucial part in the dynamics of the system. For instance, it has been shown that the population transfer to the excited state can be optimized by choosing the shape of the pulse that improves the nonadiabatic transitions [4]. It has also been shown that propagation of ultrashort laser pulses in a resonant atomic medium leads to strong reshaping effects because of dispersion [5,6]. These effects are generally considered as harmful because they distort the shape of the output pulse without any possibility of control. Here, we show how we can control the shape of a weak, resonant, ultrashort pulse propagating in an assembly of two-level atoms driven by a strong off-resonant ultrashort pulse (time duration smaller than relaxation and Doppler dephasing times).

The situation of a bichromatic field has been deeply investigated but was essentially limited to the case where a strong nonresonant driving field brings the system to a stationary state that is probed by a weak field. A large amount of literature is devoted to the spectral modifications that are induced [7–12] and only little work deals with transient effects [13]. These studies focus generally on the absorption spectra and its modification in several different configuration (two intense pump beams [8], strong probe beam [9], phase dependence when the pump and probe are mutually coherent [10], two-level degenerated system [11], transient evolution of the absorption spectra when long pulses are used instead of monochromatic waves [13],...). In comparison, only few studies were devoted to the dispersive effects [12]. The situation considered in this paper—where an ultrashort strong nonresonant pulse modifies the propagation of a weak resonant ultrashort pulse in an optically thick medium—has not been investigated. In our case, absorption is negligible and the dynamics is dominated by the transient effects induced by the strong pulse. It modifies dramatically the dispersive behavior of the medium and the temporal and spectral shape of the weak pulse is modified as a consequence. Moreover, we will show that these effects may induce a temporal modulation in the weak pulse envelope that maps out the light shifts while reducing efficiently the distortion of this pulse at long times. The modulation characteristics can be controlled by adjusting the optical depth and the relative pulse duration. The atomic media driven by the strong nonresonant pulse acts thus like a real "pulse-shaper" device operating directly in the time domain [14]. This work is a direct extension of that done in a three level ladder system where we have shown that transient light shifts induced by a strong nonresonant pulse on the upper transition can induce modulations on the temporal shape of a weak pulse that is resonant on the lower transition [15]. We will see in this paper, how these ideas can be implemented in a two-level system which is paradoxally more complex to analyze. Indeed, both the ground and excited states experience light shifts and the geometrical configuration, as explained later, requires noncollinear beams to avoid nonadiabatic effects and for spatial separation. We will give in this paper a complete analysis of this effect in a two-level system, and detail the role of various physical parameters in the shaping effect.

Finally, some aspects of this work can be related to EIT (electromagnetic induced transparency) phenomena [16] that hold generally in a three-level system for long pulses. In the case where the strong pulse has a time duration larger than that of the weak pulse and strong enough to induce light shifts larger than the weak pulse spectrum, this latter is shown to propagate without any distortion insuring a total transparency of the medium (neither dispersion or absorption). However, none of the consequences on the possibility of slowing and storing light [17] can be applied here.

The paper is organized as follows. In Sec. II, we describe in detail the phenomena that appear when a strong nonresonant ultrashort pulse (referred to as the driving pulse) interacts with a two-level system in the optical dense regime within the rotating wave approximation (RWA) approximation. In Sec. III, we consider a weak resonant pulse (the propagating pulse) which propagates in the driven atomic system. The two beams cross with a small angle between them and we concentrate on the physics of the temporal shaping of the propagating pulse. The modulation obtained is interpreted as an interference process between the incident field and the radiated field whose frequency sweeps in time because of the light shift. Finally in Sec. IV, we summarize the main results obtained and give some perspective and possible applications for pulse shaping.

II. DRIVEN TWO-LEVEL SYSTEM

We consider a two-level system with states $|a\rangle$ and $|b\rangle$ and with energies 0 and $\hbar\omega_0$. The system is driven by a strong ultrashort pulse whose expression is:

$$E_d(z,t) = \frac{1}{2}\varepsilon_{0d} f_d(z,t) e^{-i(\omega_d t - k_d z)} + \text{c.c.} \tag{1}$$

ε_{0d} is the field amplitude and f_d is the envelope of the pulse. We designate by c.c. the complex conjugate. Throughout this paper, we consider that the envelope of the pulse is real at the entrance and expresses as $f_d(z=0,t)=\frac{1}{\sqrt{\pi}}e^{-(t/\tau_d)^2}$ where τ_d represents the temporal width of the pulse at the entrance and τ_d^{-1} is the spectral bandwidth of the pulse. The central frequency of the pulse ω_d is detuned from the resonance ω_0 and $\omega_d=k_d c$. We introduce dimensionless time and space variables Z and T as $T=(t-z/c)/\tau_d$ and $Z=z/L$. Here, L is the length of the sample through which the pulse propagates. Dimensionless forms of the frequencies are $W_d=\omega_d\tau_d$, $W_o=\omega_o\tau_d$. The wave function of the system can be written:

$$|\psi\rangle(Z,T) = a(Z,T)|a\rangle + b(Z,T)e^{-iW_d T}|b\rangle. \tag{2}$$

Using the Schrödinger equation and within the rotating wave approximation (RWA), we obtain the following equations for the evolution of atomic quantities $\left(\partial_T \equiv \frac{\partial}{\partial_T}\right)$:

$$i\partial_T\begin{pmatrix} a \\ b \end{pmatrix}(Z,T) = \begin{pmatrix} 0 & -\theta_d f_d^*/2 \\ -\theta_d f_d/2 & \Delta \end{pmatrix}\begin{pmatrix} a \\ b \end{pmatrix}(Z,T). \tag{3}$$

Here $\Delta=(\omega_0-\omega_d)\tau_d$ is the dimensionless detuning and $\theta_d=\mu\varepsilon_{0d}\tau_d/\hbar$ is the usual pulse area that characterizes the strength of the pulse. The propagation of the pulse obeys the Maxwell equations. Neglecting the diffraction effects, the Doppler effect and within the slowly varying envelope approximation, the electric field evolves as follows [18]:

$$\frac{\partial}{\partial Z} f_d = i\frac{e_{disp}}{\theta_d} a^* b. \tag{4}$$

The dimensionless coefficient $e_{disp}=\frac{n\mu^2\omega_d}{2c\varepsilon_0\hbar}L\tau_d$ characterizes the severity of propagation effects on the $|a\rangle-|b\rangle$ transition and depends on the density of atoms n and the oscillator strength through the square of the dipole moment μ^2. Moreover, introducing the coefficient of absorption at resonance $\alpha_0=\frac{n\mu^2\omega_d}{2c\varepsilon_0\hbar\Delta_d}$, where Δ_d is the Doppler width, and the optical depth parameter $\alpha_0 L$, we have the relation $e_{disp}=\alpha_0 L\Delta_d\tau_d$. The quantity $\alpha_0 L\Delta_d$ represents the spectral domain around the resonance over which the dispersion affects the spectral phase of the incident pulse [19]. Thus, $e_{disp}=\alpha_0 L\Delta_d\tau_d$ can be interpreted as the ratio between this spectral range and the spectral bandwidth of the pulse.

Generally, the solution of Eq. (3) cannot be derived analytically for an arbitrary shaped pulse in the nonresonant situation ($\Delta\neq 0$) whereas the result is straightforward for a resonant pulse ($\Delta=0$) with a real envelope. Well known Rabi oscillations arise and the asymptotic value of the amplitudes depends on the pulse area θ_d. Note that the pulse area is proportional to the Fourier transform of the field at the central laser frequency.

The modification of the pulse through propagation is due to the radiation induced by the coherence a^*b as shown by Eq. (4). For a pulse far from resonance, the coherence is strongly reduced and the distortion of the pulse is small (unless the density n is very high). For a resonant pulse in the weak field regime ($\theta_d \ll 1$), we get $|a^*b| \leqslant \theta_d/2$ for $T\to\infty$ and the distortion of the field becomes important when $e_{disp}\geqslant 1$. This latter inequality means that dispersion alters the phase of all the spectral components of the incident pulse and so propagation effects can not be neglected. For a resonant pulse in the strong field regime ($\theta_d \geqslant 1$), the amplitude of the coherence can not exceed its maximum value $\frac{1}{2}$ and the propagation effects are small when $\theta_d \gg e_{disp}$ (even if $e_{disp} \geqslant 1$). Note that, the absorption is always negligible for ultrashort pulses since their spectral bandwidth is much larger than the Doppler width [19].

A. Adiabatic description

An alternative description of the interaction in which the effect of the field in the nonresonant case is clearly exhibited is possible with the use of the adiabatic basis (eigenbasis of fully perturbed Hamiltonian within the RWA). The behavior of adiabatic states has been discussed exhaustively in the literature and is of textbook knowledge [6,20]. We recall here some of the important properties.

We define the new basis *at the entrance of the medium* by the following transformation:

$$|-\rangle(T) = \cos\phi(T)|a\rangle + \sin\phi(T)e^{-iW_d T}|b\rangle,$$

$$|+\rangle(T) = -\sin\phi(T)|a\rangle + \cos\phi(T)e^{-iW_d T}|b\rangle \tag{5}$$

with ϕ given by

$$\tan(2\phi) = \frac{\theta_d}{\Delta} f_d(0,T). \tag{6}$$

In the new basis the wave function can be written

$$|\psi\rangle(Z,T) = \alpha_-(Z,T)|-\rangle(T) + \alpha_+(Z,T)|+\rangle(T). \tag{7}$$

The adiabatic description *with the adiabatic states defined at the entrance* allows us to concentrate all the Z dependence of the field and the atomic quantities in amplitudes α_+ and α_-. The amplitudes in the two basis set are related by the following relations [Eqs. (2), (5), and (7)],

$$a(Z,T) = -\alpha_+(Z,T)\sin\phi(T) + \alpha_-(Z,T)\cos\phi(T), \quad (8a)$$

$$b(Z,T) = \alpha_+(Z,T)\cos\phi(T) + \alpha_-(Z,T)\sin\phi(T). \quad (8b)$$

The amplitudes α_+ and α_- evolve according to the equation [Eqs. (3) and (8)]

$$i\partial_T\begin{pmatrix}\alpha_-\\ \alpha_+\end{pmatrix} = A\begin{pmatrix}\alpha_-\\ \alpha_+\end{pmatrix} \quad (9a)$$

with

$$A = \begin{bmatrix} -\frac{\sin 2\phi}{4}\theta_d(f_d+f_d^*) + \Delta\sin^2\phi & i\partial_T\phi + \frac{1}{2}(\theta_d(f_d\sin^2\phi - f_d^*\cos^2\phi) + \Delta\sin 2\phi) \\ -i\partial_T\phi + \frac{1}{2}(\theta_d(f_d^*\sin^2\phi - f_d\cos^2\phi) + \Delta\sin 2\phi) & \frac{\sin 2\phi}{4}\theta_d(f_d+f_d^*) + \Delta\cos^2\phi \end{bmatrix}. \quad (9b)$$

At the entrance of the sample we have $f_d(0,T)=f_d^*(0,T)$ and so Eq. (9a) simplifies to:

$$i\partial_T\begin{pmatrix}\alpha_-\\ \alpha_+\end{pmatrix} = \begin{bmatrix}(-\Omega+\Delta)/2 & i\partial_T\phi \\ -i\partial_T\phi & (\Omega+\Delta)/2\end{bmatrix}\begin{pmatrix}\alpha_-\\ \alpha_+\end{pmatrix}. \quad (10)$$

Here, Ω is the dimensionless generalized Rabi frequency defined as $\Omega=\sqrt{\theta_d^2 f_d^2+\Delta^2}$. The diagonal terms $\frac{1}{2}(\Delta\pm\Omega)$ represent the adiabatic energy levels and $\partial_T\phi$ is the nonadiabatic coupling which depends strongly on the shape of the pulse. Ω gives the instantaneous separation of the adiabatic levels becoming Δ as T approaches $\pm\infty$. The adiabatic levels experience a transient light shift during the action of the driving pulse.

In the resonant case $\Delta=0$, $\Omega=\theta_d f_d$, $\phi=\pi/4$, and $\partial_T\phi=0$. Initially, the population is equally distributed between the two adiabatic states, i.e., $\alpha_\pm(T\to-\infty)=\mp 1/\sqrt{2}$ and at time T the amplitudes are given by the expression $\alpha_\pm(T) = \mp 1/\sqrt{2}e^{(\mp i\theta_d/2)\int_{-\infty}^{T} f_d dT'}$. The population in the states $|a\rangle$ and $|b\rangle$ which are linear superposition of the adiabatic states exhibits Rabi oscillations.

In the nonresonant case and when the off-diagonal term can be neglected, the evolution is said to be adiabatic. The system starts from stationary states at $T\to-\infty$, i.e., $|-\rangle(T\to-\infty)=|a\rangle$ and $|+\rangle(T\to-\infty)=e^{-iW_dT}|b\rangle$. The driving pulse introduces new states during the transient time and as $T\to\infty$, the system moves back to the original configuration. If initially all the population is in the ground state $|a\rangle$, during the transient time some population appears in the state $|b\rangle$, but at the end of the pulse all population moves back to the ground level. The important feature of this evolution is that there is no transfer of population to state $|+\rangle$. However, in the presence of a nondiagonal coupling term, there can be nonadiabatic transitions to the adiabatic state $|+\rangle$ that results in asymptotic population in state $|b\rangle$. The nonadiabaticity of the excitation process is usually characterized by evaluating the inverse Massey "parameter" defined as the ratio between the coupling term $\partial_T\phi$ and the generalized dimensionless Rabi frequency Ω [4,21]:

$$M^{-1} = \partial_T\phi/\Omega. \quad (11)$$

For $M^{-1}\ll 1$, the evolution can be considered as adiabatic and the system experiences only light shifts. Otherwise, the interaction leads also to nonadiabatic population transfer that depends strongly on the shape of the pulse through $\partial_T\phi$ [4].

B. Behavior of the driving pulse during propagation.

During propagation, the strong nonresonant pulse is only slightly distorted but new frequency components are generated. Figure 1 shows the modification of the spectrum for the pulse with $\theta_d=60$ and $\Delta=10$ when it propagates in a medium with $e_{disp}=1$. The curve in the dotted line represents the spectrum at the entrance. The curve in the solid line represents the spectrum at the exit. New frequency components appear in the form of an oscillatory structure that can be understood by looking at the adiabatic representation (Fig. 2). In addition to the central laser frequency W_d, new characteristic

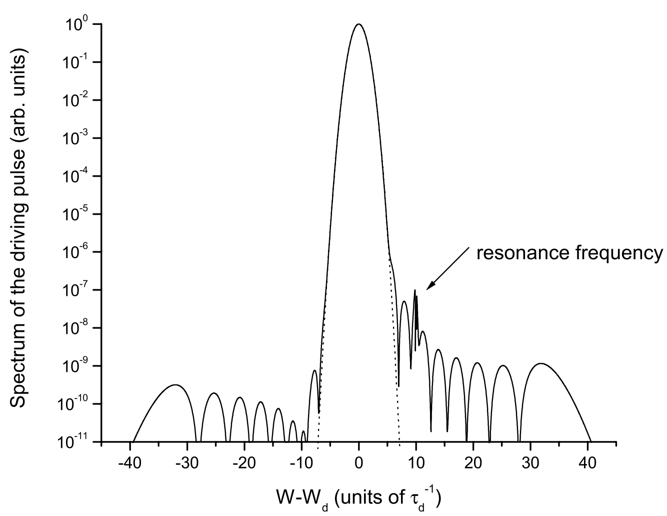

FIG. 1. Incident (dotted line) and transmitted (solid line) intensity spectrum of the driving pulse. Each frequency is created at two times giving rise to interference effects. The parameters are $\theta_d=60$, $\Delta=10$, $e_{disp}=1$. The position of resonance is marked.

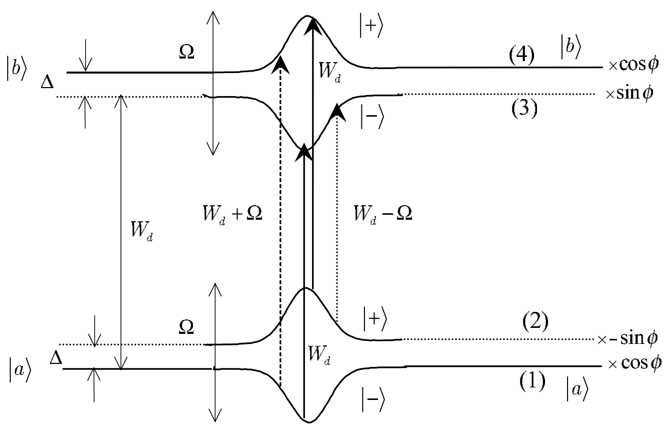

FIG. 2. Adiabatic representation: each stationary state can be decomposed as a linear superposition of the two adiabatic states with time dependent energies. Three resonance frequencies appear at W_d (solid arrows), $W_d+\Omega$ (dashed arrow), $W_d-\Omega$ (dotted arrow).

frequencies at $W_d+\Omega$ and $W_d-\Omega$ appear. This structure is analogous to the Mollow triplet, studied in the monochromatic case [3]. When dealing with pulses, the instantaneous position of the peaks is time dependent through the generalized dimensionless Rabi frequency $\Omega(T)$. The two side peaks sweep from the initial values $W_d\pm\Delta$ to the maxima $W_d\pm\sqrt{\theta_d^2/\pi+\Delta^2}$ at $T=0$ and then return back to their initial positions when the pulse vanishes. Each frequency in these bands (high and low) appears twice, so the two interfere and give the pattern shown in the figure. The extrema are located around $W_d\pm 35$ in accordance with the numerical simulations of Fig. 1.

One important remark has to be noted. The new frequencies are created because nonadiabatic transitions allow the excitation of the state $|+\rangle$, ensuring a nonvanishing value for the radiating coherence between the levels $1\leftrightarrow 4$ and $2\leftrightarrow 3$. The low and high frequency components arise during the transient time only, and when the pulse ends, the atoms continue to radiate at the resonance frequency provided there has been some population transfer to the excited state $|b\rangle$. The radiated electric field occurs even for long times after the end of the incident pulses. The radiated field associated with all these frequencies is small in comparison with that of the driving pulse but it can modify substantially the spectrum of a weak resonant pulse that propagates in the system. In the next paragraph we will show how the effects described here (light shifts and nonadiabatic transitions), modify the properties of a resonant propagating weak pulse.

III. PROPAGATION OF A RESONANT WEAK ULTRASHORT PULSE IN THE DRIVEN ATOMIC SYSTEM

In the section, we again consider that the atomic system is driven by the strong nonresonant pulse and we introduce another ultrashort resonant weak pulse that propagates in the system. The goal here is to study to what extent the modifications induced by the driving pulse in the system influence the properties of the weak pulse. The driving pulse induces light shifts and nonadiabatic effects but we are specifically interested in the shaping effects on the weak pulse induced by transient light shifts. *During propagation the driving pulse is only slightly distorted but, the nonadiabatic transitions induce new frequency components that even if they are small with respect to the strong field component, can be comparable or more significant than those of the weak pulse masking the shaping effects obtained with light shifts*. Indeed, these conditions—strong light shifts and weak nonadiabatic effects—are not easy to satisfy simultaneously since important light shifts are induced for small detuning that increases the nonadiabatic coupling. We will show that an excitation configuration in which a small angle is introduced between the two beams, overcomes this problem. In this situation, the propagation effects on the driving pulse can be neglected and this latter can be considered as uniform in the sample.

A. Equation of propagation

We assume that at the entrance of the medium, the propagating resonant pulse is coherent with the nonresonant driving pulse but has a different direction of propagation. Experimentally, it is possible to have two coherent pulses with different central frequencies in several manners, e.g., using Raman [22] or pulse shaping techniques [14]. The spatial configuration as shown later reduces the influence of the nonadiabatic transitions due to the driving pulse on the propagating pulse. We assume also that the angle between the wave vectors is small enough to use the one dimensional approximation (see Sec. III D). We introduce the weak field in the system as follows:

$$E_p(\vec{r},t)=\frac{1}{2}\varepsilon_{0p}f_p(z,t)e^{-i(\omega_0 t-\vec{k}_p\vec{r})}+\text{c.c.} \tag{12}$$

ε_{0p} is the field amplitude (real) and f_p is the envelope of the pulse defined at the entrance of the medium. We take the same pulse shape for both pulses but the two can have different pulse duration. Then we can write:

$$f_p(z=0,t)=f_d(z=0,t/\tau_{pd})e^{i\beta}, \tag{13}$$

where $\tau_{pd}=\tau_p/\tau_d$ is the ratio between the duration of the propagating and the driving pulse and β is the phase shift between the two coherent pulses. We consider next that:

$$\Delta,M \gg 1. \tag{14}$$

The Schrödinger equation in the adiabatic state representation now becomes:

$$i\partial_T\begin{pmatrix}\alpha_-\\ \alpha_+\end{pmatrix}=(A+V)\begin{pmatrix}\alpha_-\\ \alpha_+\end{pmatrix} \tag{15}$$

with $V=V^{(+)}e^{i\delta\vec{k}\vec{r}}+V^{(-)}e^{-i\delta\vec{k}\vec{r}}$ the perturbation matrix due to the weak field and $V^{(+)}$ is given by:

$$V^{(+)} = \frac{\theta_p}{2\tau_{pd}} f_p e^{-i\Delta T} \begin{pmatrix} -\frac{\sin 2\phi}{2} & \sin^2\phi \\ -\cos^2\phi & \frac{\sin 2\phi}{2} \end{pmatrix} \quad (16)$$

and $V^{(-)}=(V^{(+)})^{\dagger}$. Here, $\delta\vec{k}=\vec{k}_p-k_p\vec{e}_z$, and $\theta_p=\mu\varepsilon_{0p}\tau_p/\hbar$ represents the pulse area of the propagating pulse. In this representation, the perturbation matrix has both diagonal and nondiagonal terms that depend on both the driving and the propagating pulses. In the presence of the driving pulse the dipole moment felt by the propagating pulse is modified. The diagonal terms induce self-phase modulation. These contributions are small when compared to the light shift as long as the propagating field is weak ($\theta_p \ll 1$).

The spatial periodicity of the excitation allows the use of the Floquet theorem [23] and the series expansion of the amplitudes as follows:

$$\alpha_-(\vec{r},T) = \sum_{m=-\infty}^{m=+\infty} \alpha_-^{(m)}(Z,T)e^{im\delta\vec{k}\vec{r}}, \quad (17a)$$

$$\alpha_+(\vec{r},T) = \sum_{m=-\infty}^{m=+\infty} \alpha_+^{(m)}(Z,T)e^{im\delta\vec{k}\vec{r}}. \quad (17b)$$

The Floquet expansion is known to simplify considerably the analysis of the interaction when the excitation is periodic. This is for instance the case in solid state physics (Bloch expansion [24]) and in quantum optics when the excitation is realized beyond the RWA regime [6,25]. In the perturbative regime, the coherence can be developed up to the first order as [Eqs. (8a) and (8b)]:

$$a^*b \simeq \rho_d + \rho_p e^{i\delta\vec{k}\vec{r}} + \rho_p{}' e^{-i\delta\vec{k}\vec{r}}. \quad (18)$$

ρ_d, ρ_p, and ρ_p' are responsible for the radiation in the direction of the driving pulse $\vec{k}_d$, propagating pulse $\vec{k}_d+\left(\delta\vec{k}+\frac{\Delta}{c\tau_d}\vec{e}_z\right)$ and the symmetric direction $\vec{k}_d-\left(\delta\vec{k}+\frac{\Delta}{c\tau_d}\vec{e}_z\right)$, respectively (the $\frac{\Delta}{c\tau_d}\vec{e}_z$ term comes here from the use of the reduced time $T\propto t-z/c$ instead of the real one). The expression of ρ_d and ρ_p are given by:

$$\rho_d = \frac{\sin(2\phi)}{2}(|\alpha_-^{(0)}|^2-|\alpha_+^{(0)}|^2) + \cos^2(\phi)\alpha_-^{(0)^*}\alpha_+^{(0)} - \sin^2(\phi)\alpha_-^{(0)}\alpha_+^{(0)^*}, \quad (19a)$$

$$\rho_p = \frac{\sin(2\phi)}{2}(\alpha_-^{(0)^*}\alpha_-^{(1)} + \alpha_-^{(-1)^*}\alpha_-^{(0)} - \alpha_+^{(0)^*}\alpha_+^{(1)} - \alpha_+^{(-1)^*}\alpha_+^{(0)}) - \sin^2(\phi)(\alpha_-^{(1)}\alpha_+^{(0)^*} + \alpha_-^{(0)}\alpha_+^{(-1)^*}) + \cos^2(\phi)(\alpha_-^{(0)^*}\alpha_+^{(1)} + \alpha_-^{(-1)^*}\alpha_+^{(0)}). \quad (19b)$$

The equations of propagation for the two fields can now be written:

$$\partial_Z f_d = i\frac{e_{disp}}{\theta_d}\rho_d, \quad (20a)$$

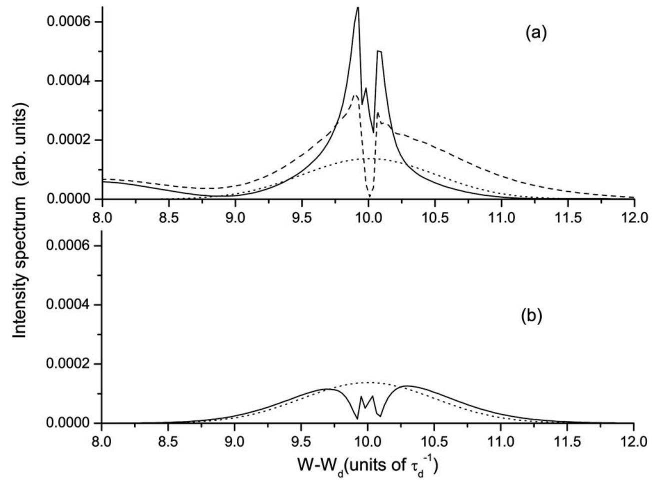

FIG. 3. Intensity spectrum of the field emitted in the direction of the propagating pulse in (a) collinear and (b) noncollinear cases. Parameters are $\theta_d=60$, $\theta_p=0.01$, $\Delta=10$, $\tau_{pd}=2$, $e_{disp}=0.5$. In both cases dashed and solid lines correspond to $\beta=0$ and π, respectively whereas the incident spectrum is represented in dotted line. In (b), the curves for $\beta=0$ and π are indistinguishable.

$$\partial_Z(f_p e^{-i\Delta T}) = i\frac{e_{disp}}{\theta_p}\tau_{pd}\rho_p. \quad (20b)$$

These relations imply that the frequencies radiated by nonadiabatic transitions (contained in the ρ_d term) are emitted in the direction of the driving pulse and therefore they do not interfere with the propagating pulse components. On the other hand, in the limit of relation (14) the dependence of the coherence ρ_p on the driving pulse is mainly due to the induced light shifts and the nonadiabatic terms play only a minor role. In the noncollinear configuration, the propagating pulse is immune to nonadiabatic effects. We show in Fig. 3, the transmitted spectrum in the direction of the propagating pulse around the atomic resonance when the two beams are collinear or not. The strength of the propagating pulse is chosen so that its spectrum intensity is comparable to the contribution due to nonadiabatic transitions (e.g., $\theta_p f_p/2\tau_{pd} \simeq |\partial_T\phi|$). In the collinear case, the nonadiabatic effects modify significantly the behavior of the propagating pulse producing an interference process that depends strongly on the phase shift, whereas these interference effects vanish in the noncollinear case. This shows that the frequencies radiated by nonadiabatic transitions are eliminated from the spectrum. The modification of the transmitted spectrum in this latter case is due to light shifts only (cf. Sec. III C). Finally, an important remark concerning the energy of the transmitted pulse can be made. We have assumed throughout this paper that the absorption in the medium is negligible. However, an exchange of energy between the driving and the propagating pulse is possible. In our situation (noncollinear beams), this latter effect is taken into account implicitly in our simulations but is found to be negligible because the nonadiabatic effects are small as explained above.

B. Transmitted intensity for the propagating pulse

From Eqs. (15), (16), (17a), and (17b), we get the following equations for the amplitudes $\alpha_\pm^{(m)}, m=0,\pm 1$:

$$i\partial_T\begin{pmatrix}\alpha_-^{(0)}\\ \alpha_+^{(0)}\end{pmatrix} = A\begin{pmatrix}\alpha_-^{(0)}\\ \alpha_+^{(0)}\end{pmatrix}, \tag{21a}$$

$$i\partial_T\begin{pmatrix}\alpha_-^{(\pm1)}\\ \alpha_+^{(\pm1)}\end{pmatrix} = A\begin{pmatrix}\alpha_-^{(\pm1)}\\ \alpha_+^{(\pm1)}\end{pmatrix} + V^{(\pm)}\begin{pmatrix}\alpha_-^{(0)}\\ \alpha_+^{(0)}\end{pmatrix}. \tag{21b}$$

The expression of the coherence ρ_p in (19b) can be considerably simplified because the propagating pulse whose frequency initially matches the atomic frequency of the two-level system is no longer resonant when the driving pulse is applied. This simplification can be understood using the adiabatic representation (Fig. 2). Eight different quantum paths contribute to the coherence ρ_p. Four correspond to absorption of the propagating pulse from level 1 and 2 to 3 and 4, and the other four correspond to emission in the opposite direction. The associated oscillation frequencies are W_d $(1\leftrightarrow3, 2\leftrightarrow4)$, $W_d-\Omega(2\leftrightarrow3)$, and $W_d+\Omega$ $(1\leftrightarrow4)$ and the contribution of these paths to ρ_p is given in Eq. (19b) by the $\sin(2\phi)$, $\sin^2(\phi)$, and $\cos^2(\phi)$ terms, respectively. The propagating pulse is no longer resonant except in a specific situation corresponding to paths $1\leftrightarrow4$ and restricted to time T before and after the application of the driving pulse. This necessitates $\tau_{pd}>1$. Now if all the population is initially in the ground state (level 1), 4 is not populated during adiabatic evolution and only the absorption path $(1\rightarrow4)$ is efficiently involved. From relations (19b), the contribution K_{14} to the coherence ρ_p and corresponding to the absorption path $1\rightarrow4$ is:

$$K_{14} = \alpha_-^{*(0)}\alpha_+^{(1)}\cos^2\phi. \tag{22}$$

During propagation the nonresonant driving pulse is only slightly distorted. In this situation, we can approximate the zero order amplitudes $\alpha_\pm^{(0)}$ by their expression in the adiabatic limit at the entrance of the medium:

$$\alpha_-^{(0)}(T,Z) \simeq e^{-i\int_{-\infty}^{T}(\Delta-\Omega/2)dT'}, \tag{23a}$$

$$\alpha_+^{(0)}(T,Z) \simeq 0. \tag{23b}$$

Using relations (10), (23a), and (23b), the solution of Eq. (21b) at the entrance of the medium gives the following expression for the amplitude $\alpha_+^{(1)}$:

$$\alpha_+^{(1)}(T,Z) = -ie^{-i\int_{-\infty}^{T}(\Delta-\Omega)/2dT'}\int_{-\infty}^{T}V_{+-}^{(+)}(T',Z)e^{-i\int_{T'}^{T}\Omega dT''}dT' \tag{24}$$

with $V_{+-}^{(+)}=\langle+|V^{(+)}|-\rangle$. Using relations (22), (23a), and (24), we finally obtain:

$$K_{14} = -i\cos^2\phi\int_{-\infty}^{T}V_{+-}^{(+)}(T',Z)e^{-i\int_{T'}^{T}\Omega dT''}dT'. \tag{25}$$

The behavior of K_{14} can be explained as follows. We note by $-T_0$ and T_0 the solutions of the equation $\Omega-\Delta=\tau_{pd}^{-1}$. This time interval $[-T_0,T_0]$ represents the duration for which the light shift between the adiabatic states induced by the driving pulse is sufficiently strong to make the propagating pulse nonresonant. Using relations (16) and (25), the coherence

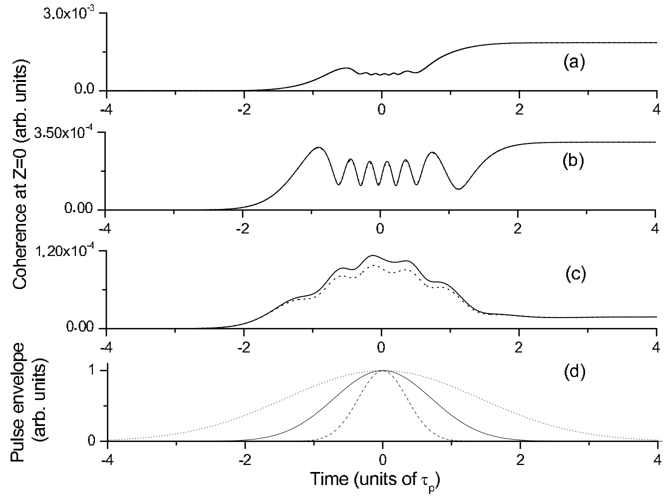

FIG. 4. Time dependence (at the entrance of the medium) of the coherence amplitude $|\rho_p|$ (solid line) and the dominant path contribution $|K_{14}|$ (dashed line) corresponding to the transition $1\rightarrow4$ of Fig. 2. Expression of $|K_{14}|$ is given by Eq. (22). Here, $\theta_d=60$, $\theta_p=0.01$, $\Delta=10$, $\beta=0$. The situations (a), (b), (c) correspond to the case $\tau_{pd}=2$, 1, and 0.5, respectively. When the propagating pulse is alone, the asymptotic value for $|\rho_p|$ is 5×10^{-3}. Finally, the difference between ρ_p and K_{14} becomes more important when the propagating pulse becomes narrower than the driving pulse. We represent in (d), the Gaussian pulse envelope of the propagating pulse in solid line (the same envelope than that of the driving pulse when $\tau_{pd}=1$), the driving pulse envelope when $\tau_{pd}=2$ (dashed line) and $\tau_{pd}=0.5$ (dotted line).

K_{14} for time T with $-T_0\leqslant T\leqslant T_0$ can be approximated by the following term corresponding to the resonant contribution that builds up from $-\infty$ to T_0:

$$K_{14} \simeq K_{14}^{(res)} = \frac{i\theta_p}{2\tau_{pd}}\cos^2\phi e^{-i\Delta T}e^{-i\int_{-\infty}^{T}(\Omega-\Delta)dT'}\int_{-\infty}^{-T_0}f_p(Z,T')dT'. \tag{26}$$

In this approximation, we have neglected the nonresonant contributions. However, these effects can be observable if we detect the radiated intensity. The interference that occurs between the resonant and nonresonant excitation amplitudes strongly modify the behavior of the radiated field intensity and the excited state population as well [15]. We represent in Fig. 4(a) the time dependence of the amplitude of the coherence $|K_{14}|$ and $|\rho_p|$ (at $Z=0$) for the parameters $\theta_d=60$, $\Delta=10$, $\tau_{pd}=2$, $\theta_p=0.01$. The amplitudes are almost identical. The amplitude $|K_{14}|$ increases initially but as the light shifts due to the driving pulse become important; it stops increasing any further. The nonresonant contribution is visible here through the oscillations that appear and that result from the interference process discussed above. When the driving pulse vanishes, the coherence amplitude increases again until the end of the propagating pulse. Note that compared to the case when the propagating pulse is alone and for which the

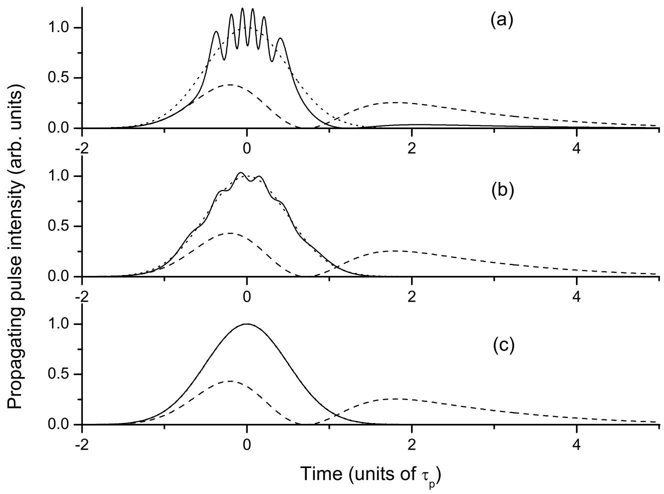

FIG. 5. Intensity envelope of the propagating pulse at the entrance of the medium (dotted line), and at the exit, in the absence (dashed line) and the presence (solid line) of the driving pulse. The situations (a), (b), (c) correspond to the case $\tau_{pd}=2$, 1, and 0.5, respectively with $e_{disp}=1/\tau_{pd}$. The others parameters are the same as in Fig. 4.

asymptotic value of the coherence amplitude is $|K_{14}|(T\gg 1) =|K_{14}^{(res)}|(T\gg 1)\simeq 5\times 10^{-3}$, the presence of the driving pulse results in a significant reduction of this asymptotic value (factor ~ 3).

The transmitted propagating field is obtained by adding the incident field to the radiated one. In Fig. 5(a) we represent the propagating pulse at the entrance of the medium (dotted line), the transmitted pulse in the absence (dashed line), and in the presence of the driving pulse (solid line). The parameters are the same as that of Fig. 4(a). Two features characterize the action of the driving pulse. First, the oscillations at long time scale, due to the atomic dispersion are strongly reduced because the driving pulse significantly reduces the coherence amplitude and thus the radiated intensity (factor ~ 9). The energy is concentrated in the central peak (pulse envelope at $T\simeq 0$) as a result of it. Second, tiny oscillations appear in this central peak. The combined action of the driving pulse and the propagation effects thus result in the transformation of a smooth pulse at the entrance of the medium into a modulated pulse at the exit. We can derive an analytical expression for the transmitted propagating pulse in the situation where the radiated field is small in comparison with the incident one. This latter condition is satisfied if the dispersion parameter is small and/or when the pulse widths of the two pulses are comparable, so that the population transferred to the excited state by the propagation pulse is substantially reduced. The atoms thus experience only the action of the incident electric field. The Z dependence of the atomic quantities a,b can then be neglected. If we restrict the value of the coherence to the resonant part of K_{14} ($\rho_p \simeq K_{14}^{(res)}$) and using Eqs. (20b) and (26), the transmitted intensity $I_p(1,T)=|\varepsilon_{0p}f_p(1,T)|^2$ can be approximated for $-T_0 \leq T\leq T_0$ at the lowest order by the following expression:

$$I_p(1,T)\simeq I_{0p}\Bigg[|f_p(0,T)|^2 - e_{disp}\cos^2\phi(T) \times\left(\cos\left(\int_{-\infty}^{T}[\Omega-\Delta]dT'-\beta\right)\right) \times\left|\int_{-\infty}^{-T_0} f_p(0,T')dT'\right|\Bigg] \tag{27}$$

with $I_{0p}=|\varepsilon_{0p}|^2$. The phase Φ_p of the transmitted pulse [with $f_p(1,T)=|f_p(1,T)|e^{i\Phi_p}$] is:

$$\Phi_p(T)=\beta+\arctan\left[\frac{A_1(T)\sin\left(\int_{-\infty}^{T_0}(\Omega-\Delta)dT'\right)}{f_p(0,T)+A_1(T)\cos\left(\int_{-\infty}^{T_0}(\Omega-\Delta)dT'\right)}\right] \tag{28}$$

with $A_1(T)=\frac{e_{disp}}{2\tau_{pd}}\cos^2\phi(T)|\int_{-\infty}^{T_0}f_p(0,T')dT'|$.

Formula (27) shows explicitly that the transmitted pulse intensity is modulated with an interference pattern which depends on the light shift induced on the transition $1\rightarrow 4$ (Fig. 2). These oscillations may be shifted by varying the relative phase-shift β. An important remark should be made here. The physical origin of these oscillations is different from those observed on the atomic quantities (excited state population and coherence). These latter originate from the interference between resonant and nonresonant contributions to the excitation probability while the oscillations observed on the transmitted pulse are the result of the interference between the incident field whose frequency is fixed and the resonant part of the radiated field whose frequency is time dependent through its light-shift dependence. These oscillations visible on the propagating transmitted pulse represent thus a mapping of the light shift in the time domain. The same phenomenon in a three-level system has been studied in detail in [15]. It can also be compared with the propagation of a chirped pulse in a two-level system, where the interference between the incident and radiated fields reveals the sweeping of the instantaneous frequency of the chirped pulse, whereas here the interference reveals the light-induced sweeping of the atomic resonance frequency [26].

An important aspect of the interaction is the enrichment of the spectrum of the propagating pulse. We represent in Fig. 6, in solid line the modification of the spectrum of the transmitted pulse for the same parameters as in Fig. 4(a). We see that the spectrum contains new frequencies. They correspond to the light shift induced on the transition $1\rightarrow 4$. These frequencies belong to a spectral band that spreads from W_d to a maximum $W_d+(\Omega(T=0)=\sqrt{\theta_d^2/\pi+\Delta^2})$. Each frequency in this band appears twice in time giving rise to interference effects as shown in the figure. Note that the part of the spectrum located within the initial profile is modified also because the radiated field interferers with the incident in this region of the spectrum.

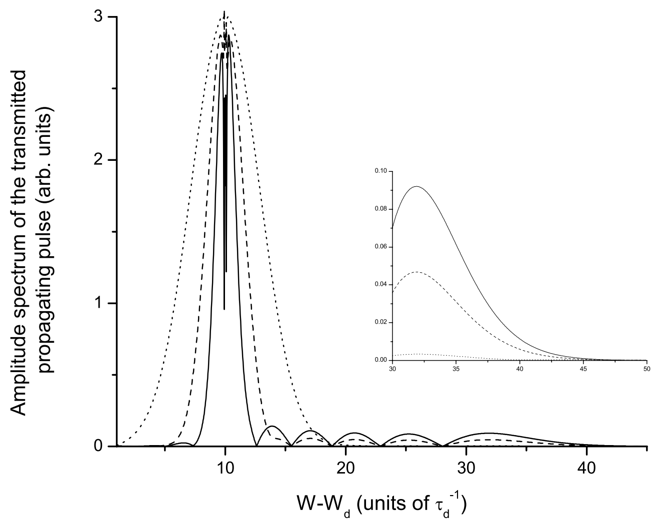

FIG. 6. Amplitude spectrum of the transmitted propagating pulse for the cases $\tau_{pd}=2$ (solid line), $\tau_{pd}=1$ (dashed line), $\tau_{pd}=0.5$ (dotted line), and $e_{disp}=1/\tau_{pd}$. The generated frequencies are more pronounced for $\tau_{pd}=2$ than the other cases. The frequency cut is the same for the three cases as shown in the inset. The others parameters are the same as in Fig. 4.

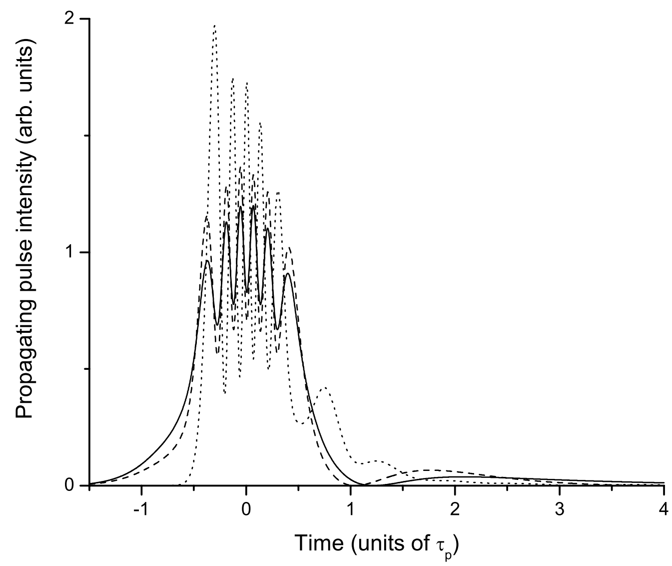

FIG. 7. Intensity envelope of the transmitted propagating pulse for $e_{disp}=0.5$ (solid line), $e_{disp}=1$ (dashed line), $e_{disp}=20$ (dotted line). Here, $\tau_{pd}=2$ and the other parameters are the same as in Fig. 4.

C. Variation with excitation parameters

The contrast of oscillations in the temporal profile can be independently varied through the dispersion parameter e_{disp} and the relative pulse duration τ_{pd} (on which depend T_0). When the relative pulse duration varies, the resonant contribution changes. For instance, if at the entrance of the medium the propagating pulse is shorter than the driving one $\tau_{pd}<1$, the light shift are important when the propagating pulse acts and the resonant part of the coherence $K_{14}^{(res)}$ vanishes ($T_0<1$). In the opposite case, when $\tau_{pd}>1$, the propagating pulse excites resonantly the system before the driving pulse freezes this interaction. The corresponding radiation induced by this nonvanishing contribution interferes with the incident field to give rise to the observed oscillations. These situations are represented in Fig. 5. In (a), is the situation discussed above with $\tau_{pd}=2$ ($\theta_d=60$, $\Delta=10$, and $\theta_p=0.01$), in (b) and (c) we have $\tau_{pd}=1$ and 0.5, respectively. For the sake of comparison, the dispersion parameters are $e_{disp}=0.5$, 1, and 2, respectively so that the coefficient $e_{disp}\,\tau_{pd}$ involved in the equation of propagation of the propagating pulse is the same for all the cases [cf. Eq. (20b)]. We see that the oscillations almost disappear as $\tau_{pd}=0.5$: the light shifts are very efficient to freeze the evolution of the system and the transmitted pulse in (c) is almost restored identical to the incident pulse. We recognize here the analogous situation of electromagnetic induced transparency for which the combination of the light-shift and the dark resonance makes the pulse insensitive to absorption [27]. In the present situation [case (c)], in addition to absorption (spectrum bandwidth much larger than the absorption width), the ultrashort pulse is immune to the dispersion and thus to propagation effects.

The behavior of the spectrum of the transmitted pulse shows also a strong dependence on the relative pulse duration. In Fig. 6, the spectral band created by light shift vanishes as τ_{pd} decreases. The frequency cutoff remains unchanged because it depends only on the strength of the driving pulse. Finally, for the same parameters as those in Fig. 5, we represent in Fig. 4 the time dependence of both $|K_{14}|$ and $|\rho_p|$ (at $Z=0$ and at same scale) for different τ_{pd} values. Here, two effects appear. First, when the propagating pulse width is reduced, the effects of light shifts are more efficient and the value of the resonant part decreases as a result. The nonresonant contribution then has an increasing relative importance that makes the interference between these two parts of the coherence more and more important. This strongly contrasts with the behavior of the oscillations of the transmitted pulse that disappear when the resonant contribution decreases. This example shows clearly the different nature of the two kinds of oscillations. Second, the difference between the coherence ρ_p and the transition amplitude K_{14} increases when the propagating pulse becomes narrower than the driving pulse. The transitions paths in the adiabatic representation of Fig. 2 that were neglected up to now, have an increasing contribution with respect of $|K_{14}^{(res)}|$ as this last one decreases. This situation highlights the complexity of the level-system structure when driven by a strong pulse.

The contrast of the oscillations can be controlled by modifying the optical depth. The modulation depth increases linearly with the dispersive parameter e_{disp} as stated by Eq. (21). In Fig. 7, the contrast increases from 18 to 33% when the dispersion parameter changes from 0.5 to 1. However, a higher value of e_{disp} leads to profound distortion of the propagating pulse profile as observed for $e_{disp}=20$: the oscillations, even if more pronounced, are shifted and irregular. In this case, the number of atoms that radiate becomes nonnegligible. The radiated field experiences ringing effects that scale in time as $(e_{disp})^{-1}$ when the propagating pulse is alone [5] and thus $(e_{disp}T_0/\tau_{pd})^{-1}$ in the presence of the driving

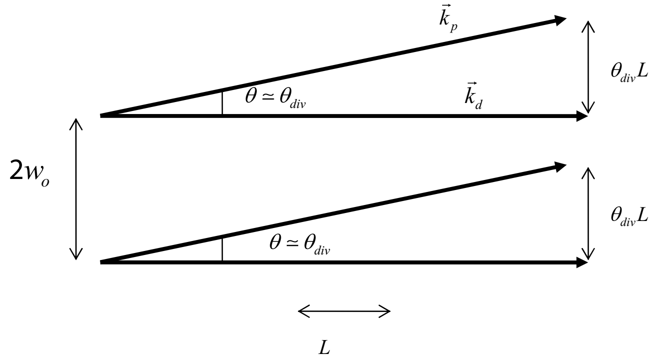

FIG. 8. Spatial configuration taking into account for the finite spatial extension of the beams.

pulse, since the number of atoms transferred is approximately reduced by a factor $(T_0/\tau_{pd})^{-1}$. When this time scale is less than τ_{pd} (e.g., τ_p in real time), the atoms feel the action of both the incident and radiated fields. Relation (27) is no longer valid and the radiated field contribute significantly to the modification of the electric field around the central peak.

D. Experimental implementation

The effects presented here can be observed for picosecond pulses in a two-level system with a large dipole moment, ensuring the induction of large light shifts without ionizing the atomic system. For instance in Rb atoms on the transition $5s\ ^2S_{1/2} \rightarrow 5p\ ^2P_{1/2}$ with $\lambda = 794.76$ nm and $\mu \simeq 1.7$ a.u. and assuming Gaussian incident pulses with $\tau_d = 10$ ps, a beam waist $w_0 = 2$ mm and an energy of 7.2 μJ, we get $\theta_d = 60$. A wavelength detuning of 0.33 nm gives $\Delta = 10$. The peak intensity is then $I \simeq 3 \times 10^6$ W/cm^2, sufficiently low to avoid direct ionization or multiphoton processes in this system. The optical depths used in the simulations presented in this paper can easily be reached. For instance for a cell with a length $L = 1$ cm (smaller than the Rayleigh length $z_0 = \frac{\pi w_0^2}{\lambda}$ $\simeq 15.8$ m), we have $e_{disp} \simeq 1$ at $n = 1.1 \times 10^{13}$ atoms/cm^3. This atomic density is obtained for a cell temperature $T \simeq 100$ °C. The Doppler width $\Delta_d = \sqrt{\frac{2k_B T}{m_{Rb}\lambda^2}}$ has a value of 0.37 GHz. The dipole dephasing time is then $\frac{\Delta_d^{-1}}{\pi} \simeq 0.86$ ns much larger than the typical characteristic time here ($\tau_d = 10$ ps) ensuring that the energy deposition in the medium is small as assumed in this paper.

The approximations used in this paper rely also on the use of a one-dimension model for the propagation (Fig. 8). The two beams cross with a small angle that should be just higher than the natural divergence angle of the beams so spatial separation can be possible. Our treatment is valid if this angle is very small (so $\theta_{div} = \lambda/\pi w_0 \ll 1$) and the spatial overlap between the two beams is perfect along the sample, e.g., $\theta_{div} L \ll w_0$. This latter condition is equivalent to having a Rayleigh length $z_0 = \pi w_0^2/\lambda$ higher than the sample length $(z_0/L \gg 1)$. In conclusion, one has to use beams with large transversal dimensions and to introduce a separation angle of the same order of the natural divergence. For the parameters given above, we get $\theta_{div} = 0.13$ mrad and the ratio z_0/L is 1.58×10^{-3}.

IV. CONCLUSION AND PERSPECTIVES

We have studied in this paper the reshaping effects that a weak resonant pulse experiences when propagating in an optically dense assembly of two-level atoms driven by a strong nonresonant ultrashort pulse. When the two beams cross, the propagating pulse is insensitive to the nonadiabatic effects induced by the driving pulse but its temporal shape is strongly affected by the light shifts. In the adiabatic representation, we identify the radiation emitted on the transition connecting the two extremely shifted levels (1 and 4 in Fig. 2) as the one responsible for this effect. The other transitions were shown to give only small nonresonant contributions to the radiating field. The shape of the transmitted pulse depends strongly on its duration with respect to the driving pulse. When it is longer, an important modulation is exhibited in the temporal profile that maps out the light shift induced by the driving pulse while the long time range tail is significantly reduced. When the driving pulse is longer, the light shifts prevent the propagating pulse from interacting efficiently with the atomic system and the propagating pulse is transmitted with almost no distortion. The medium becomes transparent to the propagating pulse in this latter case.

In addition to the possibility given by this method to measure the light shifts by recording the transmitted profile of the propagating pulse, these results show that an optically dense two-level system driven by a strong pulse can be used as a "pulse shaper" that can modify the temporal shape of an ultrashort weak pulse. The weak pulse can be modulated with a phase that depends directly on the induced light shifts. At the same time there is a significant reduction of the long tail dispersion. Application of this method is of course limited to the shaping we can obtain through the phase induced by light shifts. Complex forms can be generated by modifying the envelope of the driving pulse to obtain different light shift and thus different output shaped pulses. Mathematically, the problem is an inversion problem for the coupled equations (27) and (28) where the quantity to determine (electric field of the strong pulse) appears in both T_0, ϕ, Ω, Δ, and β parameters. This problem can be investigated numerically through optimization methods and is under consideration. The crucial advantage of this method is the possibility to shape a pulse at a characteristic time smaller than its time duration which is not possible with standard techniques since it requires the creation of new frequencies. This method also exhibits many advantages over conventional devices [14]. The latter do not operate in the UV domain, and are indirect methods since the temporal modifications are obtained by acting in the spectral domain. Strong limitations arise because of the spectral resolution of the devices that limit generally the shaping to very short pulses and the temporal resolution lies in the picosecond range making them inadequate to shape pulses in inertial fusion experiments [28]. The method presented here allows a direct shaping in the time domain avoiding the above problems and represent an ideal complement for the conventional methods while operating in the picosecond range and/or using UV pulses. The modulation can be varied through the laser and medium characteristics (optical depth, driving pulse intensity, relative pulse durations) providing a large range of control parameters. Extension of this work to the situation where the propagating pulse is strong is an interesting perspective since the self-phase modulation may generate new spectral bands and thus complex temporal structures are expected.

[1] I. I. Rabi, Phys. Rev. **51**, 652 (1937); H. M. Gibbs, Phys. Rev. A **8**, 446 (1973).

[2] D. Grichkowsky and J. A. Armstrong, Phys. Rev. A **6**, 1566 (1972); D. Grichkowsky, *ibid.* **7**, 2096 (1973).

[3] B. R. Mollow, Phys. Rev. A **5**, 2217 (1972); F. Y. Wu, S. Ezekiel, M. Ducloy, and B. R. Mollow, Phys. Rev. Lett. **38**, 1077 (1977); P. L. Knight and P. W. Milonni, Phys. Rep. **66**, 21 (1980).

[4] P. R. Berman, L. Yan, and K.-H. Chiam, Phys. Rev. A **57**, 79 (1998).

[5] L. Allen and J. H. Eberly, *Optical Resonance and Two-level Atoms* (Wiley, New York, 1975).

[6] B. W. Shore, *The Theory of Coherent Atomic Excitation* (Wiley, New York, 1990).

[7] R. Guccione-Gush and H. P. Gush, Phys. Rev. A **10**, 1474 (1974); R. W. Boyd, M. G. Raymer, P. Narum *et al.*, *ibid.* **24**, 411 (1981); M. T. Gruneisen, K. R. Mac Donald, and R. W. Body, J. Opt. Soc. Am. B **5**, 123 (1988); M. T. Gruneisen, K. R. Mac Donald, A. L. Gaeta *et al.*, Phys. Rev. A **40**, 3464 (1989); Z. Ficek and H. S. Freedhoff, *ibid.* **53**, 4275 (1996); A. S. M. Windsor, C. Wei, S. A. Holmstrom *et al.*, Phys. Rev. Lett. **80**, 3045 (1998); T. H. Yoon and J. R. Park, Phys. Lett. A **264**, 142 (1999).

[8] T. G. Rudolph, H. S. Freedhoff, and Z. Ficek, Phys. Rev. A **58**, 1296 (1998) and references therein.

[9] N. B. Manson, C. Wei, and J. P. D. Martin, Phys. Rev. Lett. **76**, 3943 (1996); C. C. Yu, J. R. Bochinski, T. M. Kordich *et al.*, Phys. Rev. A **56**, R4381 (1997).

[10] R. E. Silverans, G. Borghs, P. De Bisschop *et al.*, Phys. Rev. Lett. **55**, 1070 (1985); Q. Wu, D. J. Gauthier, and T. W. Mossberg, Phys. Rev. A **49**, R1519 (1994).

[11] A. Lipsich, S. Barreiro, A. M. Akulshin *et al.*, Phys. Rev. A **61**, 053803 (2000).

[12] C. Wei and N. B. Manson, Phys. Rev. A **49**, 4751 (1994); R. S. Bennink, R. W. Boyd, C. R. Stroud *et al.*, *ibid.* **63**, 033804 (2001).

[13] J. E. Golub and T. W. Mossberg, Phys. Rev. Lett. **59**, 2149 (1987); N. Lu and P. R. Berman, Phys. Rev. A **36**, 3845 (1987); V. S. Egorov, V. N. Lebedev, I. B. Mekhov *et al.*, *ibid.* **69**, 033804 (2004).

[14] A. M. Weiner, Rev. Sci. Instrum. **71**, 1929 (2000).

[15] J. C. Delagnes and M. A. Bouchene, Phys. Rev. A **69**, 063813 (2004).

[16] J. E. Field, K. H. Hahn, and S. E. Harris, Phys. Rev. Lett. **67**, 3062 (1991); J. P. Marangos, J. Mod. Opt. **45**, 471 (1998).

[17] D. F. Phillips, A. Fleischhauer, A. Mair *et al.*, Phys. Rev. Lett. **86**, 783 (2001).

[18] P. W. Milonni and J. H. Eberly, *Lasers* (Wiley, New York, 1988), pp. 251–252.

[19] M. A. Bouchene, Phys. Rev. A **66**, 065801 (2002).

[20] N. V. Vitanov, J. Phys. B **28**, L19 (1995).

[21] N. F. Mott and H. S. W. Massey, *The Theory of Atomic Collisions* (Oxford University Press, Oxford, 1965), Chaps. 19 and 21.

[22] R. W. Boyd, *Nonlinear Optics* (Academic Press, San Diego, 1992).

[23] R. Grimshaw, *Nonlinear Ordinary Differential Equations* (CRC Press, Boca Raton, 1993), Chap. 3.

[24] N. W. Ashcroft and N. D. Mermin, *Solid State Physics* (Saunders, Philadelphia, 1976).

[25] J. H. Shirley, Phys. Rev. **138**, B979 (1965).

[26] J. E. Rothenberg and D. Grischkowsky, J. Opt. Soc. Am. B **2**, 626 (1985).

[27] K. J. Boller, A. Imamolu, and S. E. Harris, Phys. Rev. Lett. **66**, 2593 (1991).

[28] X. Ribeyre, C. Rouyer, F. Raoult *et al.*, Opt. Lett. **26**, 1173 (2001).